Spacer Compression for a Triple Conductor Bundle

Jean-Louis Lilien, Eric Hansenne, Konstantin O. Papailiou, *Senior Member, IEEE*, and Jürgen Kempf

***Abstract*—This paper presents recent investigations on spacer compression. It contains results of short-circuit tests on suitable instrumented spacers, comparison with advanced calculation methods and a critical review of current practice for spacer design. The main conclusion of the paper is, that in certain cases caution is needed, when designing spacers on compression by using the simple Manuzio formula available today.**

I. Introduction

SPACERS are indispensable components in the design and construction of high voltage overhead lines and outdoor substations, when bundle conductors are employed. Although they have been for many years utilized extensively, their behavior is still the subject of various investigations. This fact is documented in the existence of working groups within CIGRE and IEC engaged in their study and their standardization.

A major parameter for the mechanical strength design of spacers are the loads imposed on them by short-circuits. This is a complex dynamical phenomenon, which has been studied for a long time. In a classical Institute paper dated from 1965, [1], Manuzio described very clearly the physical background, performed short-circuit tests and developed a simple theory which gave access to spacer compression. Her formula fitted very well the test results and is still in use for the design of spacers. It is also included in the latest relevant IEC draft standard, [2].

What is often overlooked is the fact, that this formula is based on tests performed on quite long subspans (65 m), with strong anchoring and neglecting supporting structure and insulator effects. The tests were carried out without current asymmetry and for relative moderate short-circuit rms values (25 kA), which induced very small pinch (only 10% increase of the tension) on the conductors. In such configurations the formula can be applied. But actually today's spacers must withstand much higher short-circuit currents (50 kA and above), with full asymmetry and must be applicable both for overhead lines and substations. In such cases, as it is shown in the following, the formula underestimates spacer compression by a factor of two or even more.

In the meantime many investigations have been done on bundle conductors, but mainly concerning the pinch effect, i.e., the increase of the tension in the cable. For instance in a recently published CIGRE brochure, [3], which summarizes the state of the art and the background of IEC 865, [4], which itself deals with the short-circuit loading of structures in open-air substations, practically no information concerning spacer compression is given. Nevertheless actual knowledge on spacer compression has sensibly increased since 1965.

In order to clarify the situation, short-circuit tests have been performed, with the task to evaluate the behavior of spacers for a triple conductor arrangement at 40 kA short-circuit level. The tests have been conducted on relative short span lengths and moderate tensions in the conductors, so that the application of spacers in substations would also be covered.

Finally a numerical simulation has been carried out, in order first to reproduce the test results and then to extrapolate them and to extend the relevance of the method also for the application of spacers in overhead lines.

II. Test Arrangement

The phase arrangement is a triple bundle with 54/7ACSR Cardinal subconductors (546 mm^2 total cross-section, 30 mm overall diameter, 1.85 kg/m weight) and with 40 cm separation between the center of each subconductor. The short-circuit current is 40 kA/phase during 0.2 s. For design purposes, maximum asymmetry with the time constant available in the test station (46 ms) has been considered, resulting in a peak current of 100 kA.

In the test station of FGH (Forschungsgemeinschaft für Hochspannungs- and Hochstromtechnik, Mannheim-Rheinau, Germany), where the tests have been carried out, the span length was around 40 m and the spacer has been installed either at midspan (subspan length of approx. 20 m), or at the end of the span (subspan length of approx. 40 m), Fig. 1. In this latter case only half of the loading was acting on the spacer because the other subspan contribution has been "missing," a fact which had to be taken into account in the evaluation of the test results.

In an actual overhead line situation, typical subspan lengths are up to 80 m, with about 4 subspans per span.

In the test station, the tension per phase (for the three subconductors) was either 20, 40, or 60 kN which means very low sag (0.2 m at 40 kN).

In an overhead line the tension per phase (for the three subconductors) is about 90 kN (typically 20% of the conductor breaking strength) with a sag of about 8 m.

The supporting structure of the bundle was a stiff portal steel lattice structure, and the short-circuit feeding was done using specific hardware and return conductor arrangement, as shown schematically in Fig. 1.

A prototype rigid spacer has been tested with a star shape (all three spacer arms starting from the geometric center of gravity of the triangle), Fig. 2. This spacer was equipped with strain gauges in order to measure the maximum mechanical stresses during the short-circuit and from these to determine the compression forces acting on the spacer arms.

Manuscript received December 20, 1996.

J. L. Lilien and E. Hansenne are with the University of Liège, B-4000 Liège, Belgium.

K. O. Papailiou is with SEFAG, CH-6102 Malters, Switzerland.

J. Kempf is with PFISTERER, D-70327 Stuttgart, Germany.

Publisher Item Identifier S 0885-8977(00)00673-7.

In this work, six predominant disturbance categories are selected to be identified using the proposed wavelet-based neural classifier. They are high (A) and low (B) frequency capacitor switchings, perfect 60 Hz sinusoidal waveform (C), impulse transient (D), sag (E), and momentary interruption (F) disturbances. The first four disturbance types are identified in the wavelet domain, while the last two are identified in the time domain. The total number of disturbance waveforms utilized in the training and testing phase for disturbance types A, B, C, and D is 524 and 406 waveforms, respectively. The total number of waveforms for types E and F is 269 waveforms. Thus the total number of waveforms is 1199 waveforms. All disturbance waveforms are courtesy Houston Lighting and Power and were collected using BMI monitoring instrument.

The performance of the classifier in identifying disturbance types E and F is very encouraging. Using the sag and momentary interruption detector, the classifier is capable of identifying 98.5% correctly, out of 269 disturbance waveforms of types E and F.

For disturbance types A, B, C, and D, the performance of the classifier is evaluated in terms of accuracy rates and relevant probabilistic-like measures. Using the simple voting scheme decision-making method, and a threshold agreement level of 51%, the classifier is able to achieve an accuracy rate of 91.8% at the expense of rejecting 7.8% of the waveforms as ambiguous. The classifier is able to reject about 60% of the outliers. Higher performance in terms of accuracy rate can be achieved by setting a higher threshold agreement level. However, there will be more waveforms rejected as ambiguous.

Using the Dempster–Shafer theory of evidence and a lower bound threshold of a belief interval 70%, the classifier is able to achieve an accuracy rate of 92.3% at the expense of rejecting 10.8% of the waveforms as ambiguous. It is capable of rejecting about 68% of the outliers.

In this work, the voting and the Dempster–Shafer theory of evidence performs comparably since both schemes use the same evidence provided by the neural networks. However, the Dempster–Shafer theory of evidence provides a better measure of the degree of belief for the identified disturbance waveform. If a new technique is developed to specifically provide disconfirming evidence, the Dempster–Shafer will be very useful to combine disconfirming and confirming evidence. The voting scheme is unable to perform such a function.

The choice of a threshold level in the voting scheme and the Dempster–Shafer theory of evidence is determined by the performance of each threshold level in terms of accuracy rate given acceptance, rejection rate, the average agreement level (for the voting scheme), and the average lower bound of belief interval (for the Dempster–Shafer theory of evidence). For this work, the preferred threshold agreement level for the voting scheme is 51% and the preferred threshold of the lower bound of a belief interval for the Dempster–Shafer theory of evidence is 60–70%.

A slight difficulty is likely to occur in training the neural networks. The training may take a considerable amount of time depending on computing power and the size of the training data set. For example, with appropriate choice of learning function described in [1, Eq. (6)], the amount of training time for ANN's #1, #6, and #11 is less than 1 h with a 150 MHz desktop computer. Once the training phase is completed, the testing phase is very straightforward. Using the same desktop computer mentioned above, the classifier is capable of identifying one disturbance waveform within 1.6 and 1.9 s, respectively, using the voting and the Dempster–Shafer schemes.

The classifier is expected to assist power quality engineers in identifying disturbance waveforms. It may be integrated with other expert systems to provide mitigation procedures for the identified disturbance. The classifier may also be installed on a distribution feeder to investigate power quality concerns and to estimate disturbance statistics.

ACKNOWLEDGMENT

The authors are indebted to several electric utilities and their engineers (mentioned in [1]) for their generous technical support, especially to M. A. Polston of Houston Lighting and Power.

REFERENCES

[1] S. Santoso, E. J. Powers, W. M. Grady, and A. C. Parsons, "Power quality disturbance waveform recognition using wavelet-based neural classifier—Part 1: Theoretical foundation," *IEEE Trans. on Power Delivery*, vol. 15, no. 1, Jan. 2000.

[2] *Recommended Practice on Monitoring Electric Power Quality, P1159/D6*, IEEE Standards Department, Dec. 1994.

[3] C. M. Bishop, *Neural Network for Pattern Recognition*. Oxford: Oxford University Press, 1995.

Surya Santoso (S'95) received the B.S. degree from Satya Wacana Christian University, Salatiga, Indonesia in 1992, and the M.S. and Ph.D. degrees from the University of Texas at Austin in 1994 and 1996, respectively, all in electrical and computer engineering. His primarily research interests include nonstationary signal analysis, in particular time-scale and time-frequency analyzes with application to power system engineering and turbulence studies in fusion plasmas, and pattern recognition with application to power quality disturbance waveforms.

Edward J. Powers (F'83) received the B.S. degree from Tufts University, Medford, MA, the M.S degree from Massachusetts Institute of Technology, Cambridge, MA, and the Ph.D. degree from Stanford University, Stanford, CA, in 1957, 1959, and 1965, respectively, all in electrical engineering. He is currently the Texas Atomic Energy Research Foundation Professor in Engineering and Director of the Electronics Research Center at The University of Texas at Austin. His primarily professional interests lie in the innovative application of digital higher order statistical signal processing in the analysis, interpretation, and modeling of random data characterizing nonlinear physical phenomena and systems; and the utilization of wavelet transforms to detect and identify transient events in various physical systems.

W. Mack Grady (SM'83) received the B.S. degree from the University of Texas at Arlington, TX, and the M.S. and Ph.D. degrees from Purdue University, IN, in 1971, 1973, and 1983, all in electrical engineering. He is currently a Professor of Electrical and Computer Engineering at The University of Texas at Austin. His areas of interest include power systems analysis, power system harmonics, power quality, and short term load forecasting. He is the chairman of the IEEE PES General Systems Subcommittee and a registered professional engineer in Texas.

Antony C. Parsons (S'96) received the B.S. degree in electrical engineering from the University of Houston and the M.S. degree from the University of Texas at Austin in electrical and computer engineering in 1995 and 1996, respectively. He is currently is a graduate student at the University of Texas at Austin. His areas of interest include power quality and power system harmonics.

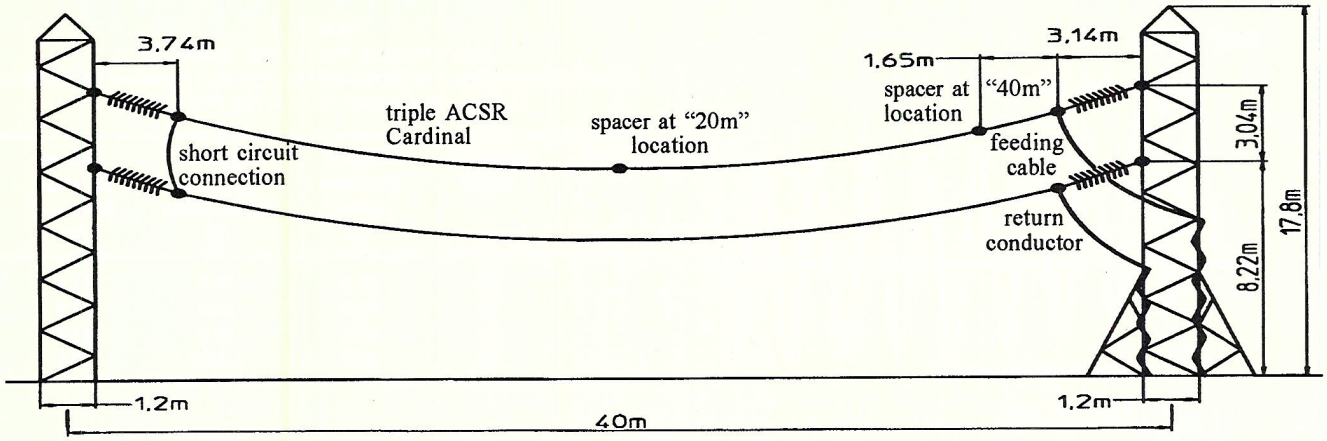

Fig. 1. Schematic of test span.

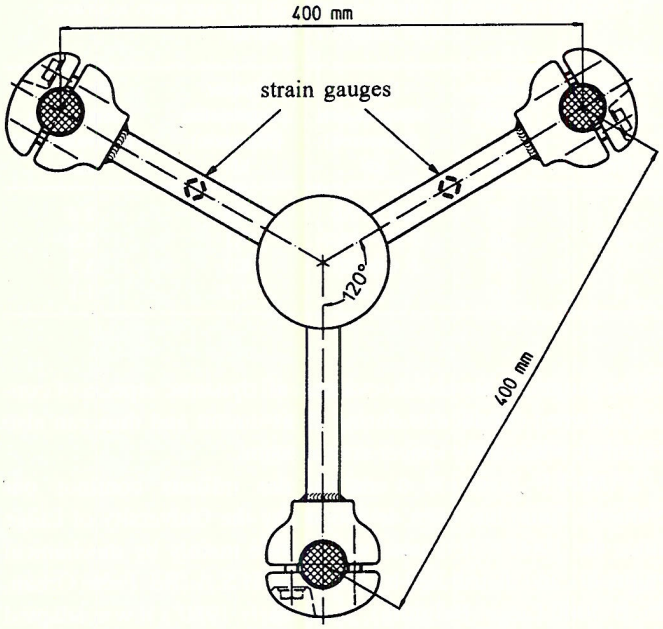

Fig. 2. Star spacer instrumented with strain gauges for measurement of the compression forces.

III. Test Results

Following results for the test with two 20 m subspans and a phase tensile load of approx. 40 kN are detailed over the first 100 ms, during which the maximum compression force occurs on the spacer, Fig. 3. Practically for all cases, peak value was observed 70 ms after short-circuit inception. As it can be seen from these curves, the phenomenon of the pinch is divided in several parts: contact, propagation toward the spacers and oscillation around a virtual static equilibrium, i.e., the static position which would be obtained if no dynamic effects would occur. As also shown in Fig. 3(b), this results in a maximum pinch during the first contact. At the end of the short-circuit progressive separation of subconductors toward the middle of the span occurs, where both waves (from each span end) are combined together and reflected to come back toward the spacer, back again to the end of the span, etc., until complete damping of the oscillations takes place. During this process, strong spacer compression is first observed, to be followed by successive traction and compression caused by the wave propagation effect. This can also be seen in Fig. 3(c), whereby traction is sensibly lower than the initial compression. As maximum compression occurs generally in the first 100 ms (70 ms in this case) after short-circuit inception, the asymmetry of the short-circuit [i.e., the presence of a pseudo-continuous current component, Fig. 3(a)] sensibly influences spacer compression.

The following Table I is a summary of the test results relating to the increase in conductor tension during short-circuit due to the pinch effect whereby in this and the following tables the values for case no. 4 are averages from two "identical" tests.

When pinch effect occurs, not only the spacer is compressed, but also the tension in the conductors themselves is increased. For example in these tests, the pinch was larger than two times the initial tension in the conductors, Fig. 3(b). Of course, spacer compression is affected by the instantaneous tension in the conductors, and not by its initial value before short-circuit, that means all factors affecting pinch, i.e., the behavior of dead-ends (stiffness, frequencies, presence of heavy insulators), will also affect spacer compression.

It is further interesting to point out in Table I, that the increase of tension in the phase, i.e., the difference between initial value and maximum pinch force, is about the same for a given subspan length, independently of initial static tension, as already pointed out in [3].

The next table, Table II, contains the comparison of the experimental values for spacer compression with the values calculated by the well known Manuzio formula.

The Manuzio formula as first given in [1], is for the sake of completeness repeated here:

$$P_{\max} = 0.46 I_{cc} (F_{st} \log(a_s/d))^{1/2}.$$

where $P_{\max}$ is the spacer compression force in kg, with I_{cc} the short-circuit current rms symmetrical value per phase in kA, F_{st} the initial static tensile load for each subconductor in kg, a_s the subconductor separation and d the diameter of a subconductor in mm. As already mentioned the Manuzio formula is independent of subspan length. The factor 0.46 takes into account the necessary adjustments for the triple bundle used here.

This formula can be converted into the international unit system:

$$P_{\max} = 1.45 I_{cc} (F_{st} \log(a_s/d))^{1/2}.$$

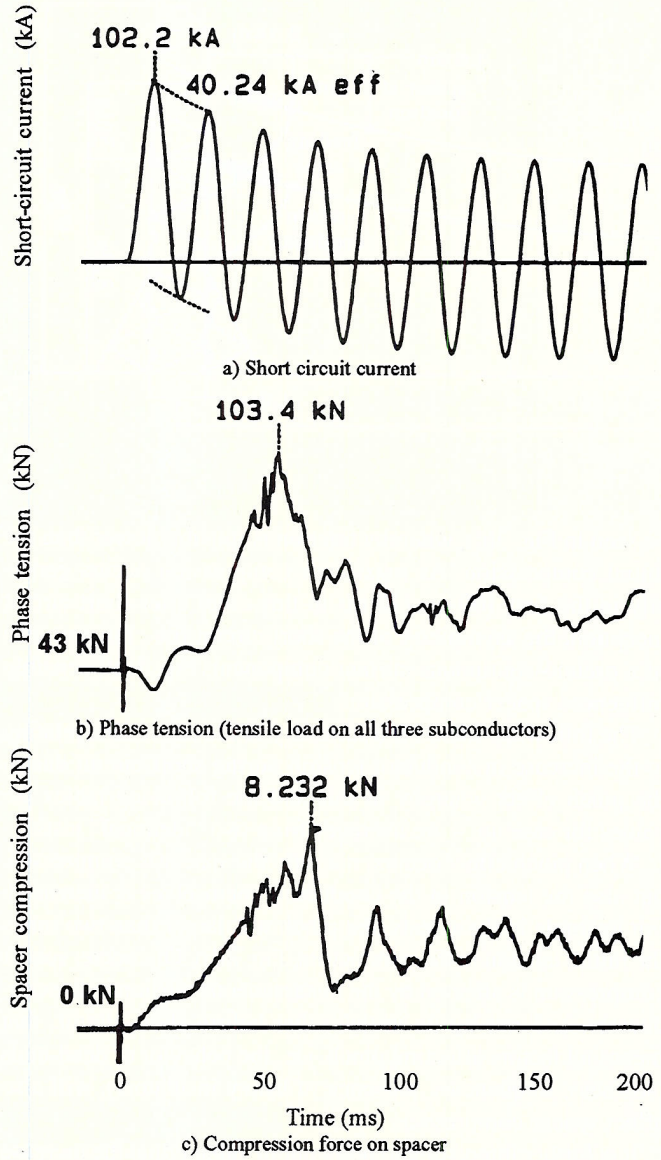

Fig. 3. Oscillograms for test no. 4 (20 m and 43 kN). (a) Short circuit current, (b) phase tension (tensile load on all three subconductors), and (c) compression force on spacer.

Therein $P_{\max}$ is in N, I_{cc} in kA, F_{st} in N, and a_s and d in mm.

In the 40 m test, the spacer was placed very close to the supporting structure. That means that the force contribution from the adjoining subspan on the spacer compression was practically missing. For this reason the measured values had to be multiplied by the factor two. Evidently spacer compression increases with initial static tension in the conductors.

Table II demonstrates clearly the shortcoming of the Manuzio formula for short and medium subspans. It underestimates spacer compression in this case up to 50% and its application can lead to border line design.

IV. Computer Simulation

A. Description of the Software

In the last years, advanced finite element software have been developed integrating short-circuit loading in cable structures.

TABLE I
TEST RESULTS WITH RIGID SPACER IN STAR CONFIGURATION ON TRIPLE ACSR CARDINAL SHOWING INCREASE IN CONDUCTOR TENSION DUE TO THE PINCH EFFECT

Test Nr.	Subspan length m	Tension per phase (initial) kN	Tension per phase (peak value) kN	Tension per phase (increase) kN
1	40	23.0	55.6	32.6
2	40	40.0	67.8	27.8
3	40	60.0	90.0	30.0
4	20	43.0	100.0	57.0

TABLE II
COMPARISON OF TESTS WITH THE MANUZIO FORMULA FOR SPACER COMPRESSION; THE MEASURED VALUES FOR THE TESTS ON THE 40 m SUBSPAN ARE MULTIPLIED BY TWO (2) TO TAKE INTO ACCOUNT THE "MISSING" SUBSPAN

Test Nr.	Subspan length m	Spacer compression (measured) kN	Spacer compression (Manuzio) kN	Spacer compression (undervaluetion) kN
1	40	2·3.5=7.0	5.4	2.6
2	40	2·5.0 =10.0	7.1	2.9
3	40	2· 6.0=12.0	8.7	3.3
4	20	8.4	7.3	1.1

These programs are able to evaluate all dynamic aspects of contact between conductors during short-circuit and thus can also calculate adequately spacer compression.

SAMCEF (systeme d'analyze des milieux continus par elements finis) has been developed by the University of Liège since the 1960's. It is used world wide mainly by mechanical engineers and distributed by SAMTECH S.A (Bd. Frére Orban, 25, B-4000 Liège, Belgium). In the early 1980's it was adapted to cable structures, noticeably with electrodynamic loading during short-circuit [5]. Completely rewritten in 1995, it now includes nonlinear cable elements (three degrees of freedom per node) and nonlinear beam elements (six degrees of freedom per node) consisting usually of two nodes. As constitutive law, Green's measure of deformation is used, while the material behavior remains linear (Hooke's law). A specific treatment is applied for contact between subconductors employing Lagrangian multipliers, with reevaluation of speed after contact. Also elements for stiffness, dampers, hinges (with blocking angle), etc., are available. The time step analysis is performed using the Hilbert–Hughes–Taylor schema. It is an implicit time-step algorithm, whereby the iteration matrix is usually refreshed at each iteration. A time-step of typically 10 ms for interphase effects and 1 ms for contact in bundle conductors is recommended, with 3–5 iterations needed for each time-step. The short-circuit nonlinear loading is reevaluated at each time step, to cover the geometric position of the complete structure and the time aspects (transients) resulting from the short-circuit current wave shape. Heating can also be included in the simulation. Typical CPU time on a Sun Sparc20 workstation, i.e., for the case examined here with one bus-bar including supporting structures, is around 10 min for interphase effects (observation

time 2 s) and one hour if contacts must be taken into account (observation time 0.1 s).

For the computer simulation of the tests described in this paper, a cable element (i.e., the bending stiffness has been neglected) has been used for the conductor, a nonlinear beam element for the supporting structure and a specific element for the spacer to take account of its rigid structure.

The time analysis has been performed with a sophisticated method to allow contact between subconductors and to consider corresponding changes in the structure when impact occurs.

The structure has been divided into small parts (the smaller one close to 3 cm) especially around the spacer to evaluate its general behavior and to include if necessary, all aspects, such as supporting structures, return cable, anchoring insulators, droppers for feeding and short-circuit connections, yoke plates, etc. Nevertheless, as usual in such computations, due to partly unknown data of the portals, some simplified assumptions had to be made. In this case supporting structures have been modeled by equivalent beams having a stiffness of 2300 N/mm on one side and 1800 N/mm on the other side and basic eigenfrequency of 3.2 Hz on one side and 5 Hz on the other side; these values have been experimentally determined in previous investigations.

B. Simulation of the Tests

The following tests have been simulated by SAMCEF:

1) Configuration with two subspans of 20 m with initial static tension of $F_{st} = 43$ kN.
2) Configuration with one subspan of 40 m with initial static tension of $F_{st} = 20$, 40, and 60 kN.

In the simulation, actual geometrical data were introduced, i.e., the true span length carrying current was close to 34 m and not 40 m. Also the 20 m case has been evaluated in fact with two 17 m subspans and the 40 m case has been evaluated with 32 in from one side of the spacer and 2 in on the other side, Fig. 1.

Table III summarizes the results from the test measurements and the computer simulations for spacer compression and peak tension per phase. Agreement is in both cases very good.

The values in brackets in Table III are calculated assuming fully rigid supporting structures. In this case the tension in the conductors rises by additional 5–15%, which influences the spacer compression accordingly.

C. Simulation of a Typical Overhead Line Situation

Since good correlation has been achieved between measurements and computations for short subspans—typical for substations—it was found promising to extend the calculation methodology to long subspans in order to cover also the range typical for overhead lines. The following cases have been pursued to better quantify the influence of subspan length and conductor tensile load and thus to evaluate by computer simulation spacer compression for the star (rigid) spacer:

1) Configuration with four subspans of 80 m with initial static tension of $F_{st} = 90$ kN. The four subspans are equal and directly connected to fully rigid anchoring points.
2) Configuration with two subspans of 20, 40 and 80 m each at a static tension per phase of 20, 40, 60 and 80 kN.

TABLE III
COMPARISON BETWEEN TESTS AND COMPUTER SIMULATIONS FOR SPACER COMPRESSION AND PEAK TENSION PER PHASE; VALUES BETWEEN BRACKETS WITHOUT SUPPORTING STRUCTURE EFFECTS; TEST BASIC DATA AS IN TABLE I

Test Nr.	Spacer compr. (measured) kN	Spacer compr. (computed) kN	Spacer compr. (deviation) %	Tension per phase (peak value) kN	Tension per phase (computed) kN
1	3.5	3.25	-7	55.6	60
2	5.0	(4.8)	-8	67.8	(110)
3	6.0	(6.0)	0	90.0	(105)
4	8.4	9.0(12.6)	+5	99.4	102(120)

TABLE IV
COMPUTED VALUES OF SPACER COMPRESSION FOR TWO AND FOUR SPAN ARRANGEMENTS WITH TRIPLE ACSR CARDINAL, SHOWING INFLUENCE OF SUBSPAN LENGTH AND TENSION PER PHASE FOR TYPICAL VALUES USED IN SUBSTATIONS AND OVERHEAD LINES; SUPPORTING STRUCTURE EFFECTS ARE NEGLECTED; THE LAST LINE SHOWS THE VALUES CALCULATED BY THE MANUZIO FORMULA (M), WHICH ARE INDEPENDENT OF SUBSPAN LENGTH

Subspan length m	Static tension per phase: 20 kN	40 kN	60 kN	90 kN
	Spacer compression (computed) in kN			
2·20	11.2	13.3	13.9	14.7
2·40	9.4	10.7	11.8	13.0
2·80	-	10.0	10.6	12.2
4·80	-	-	-	11.0
M	5.0	7.1	8.7	10.7

The simulation results are presented in Table IV.

It should be noted that for two 80 m subspans and 90 kN tension per phase, the typical overhead line case, larger (+10%) compression forces (12.2 kN) act on the spacers, when compared to the four subspan simulation (11 kN).

It is further clear from Table IV, that spacer compression increases with conductor tension and decreases with subspan length in the range examined here. Obviously above a certain value the subspan length has a second order effect in spacer compression. If this remark can be applied in most situations in overhead lines, it is certainly not the case for substations, where practical subspan lengths can easily be in the range of the critical values at which subconductor contact just takes place, as explained in [3]. The pinch effect can be increased by a factor of two or three close to that dangerous range and because of that,the compressive forces acting on the spacers rise significantly.

In Fig. 4 the curves showing spacer compression for the two subspan arrangements are presented. In this figure the values for spacer compression as calculated by the Manuzio formula are shown as straight lines, emphasizing the subspan range where undervaluation in spacer design would occur, when latter formula is used.

D. Transient Analysis of Spacer Compression and Phase Tension

To evaluate if a method of simulation is correct or not, i.e., whether it includes a good enough physical hypothesis to follow

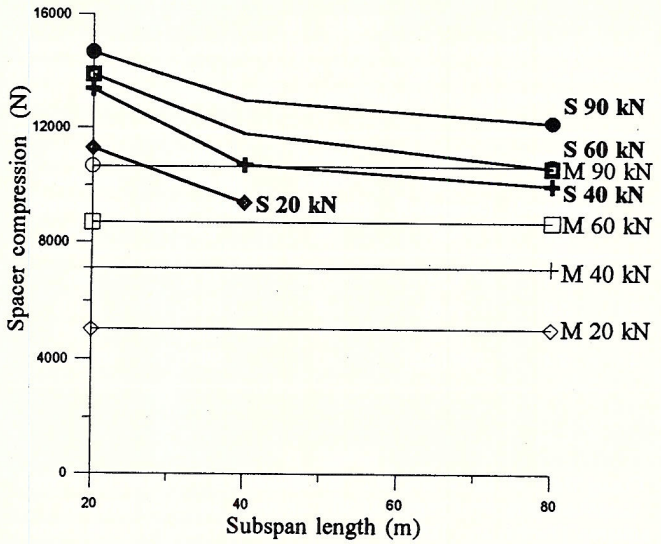

Fig. 4. Comparison of SAMCEF simulation (S, bold curves) and Manuzio formula (M, horizontal lines) for two identical subspans and different phase tensions with triple ACSR Cardinal and 40 kA rms (100 kA peak) short circuit without consideration of supports.

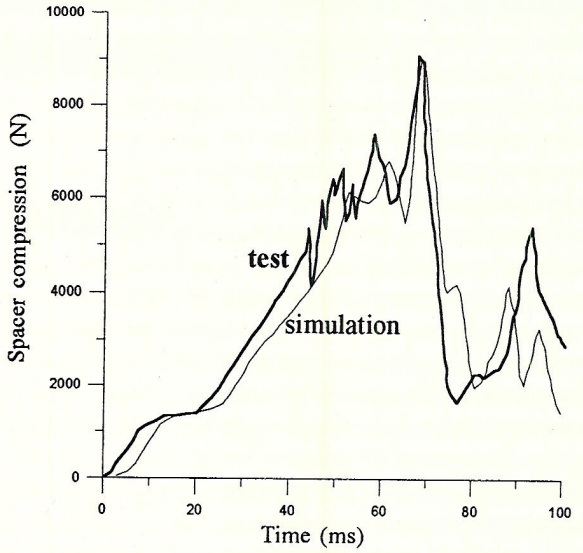

Fig. 5. Spacer compression over the first 100 ms after short circuit inception; comparison of test (bold curve) and simulation with the data of Fig. 3.

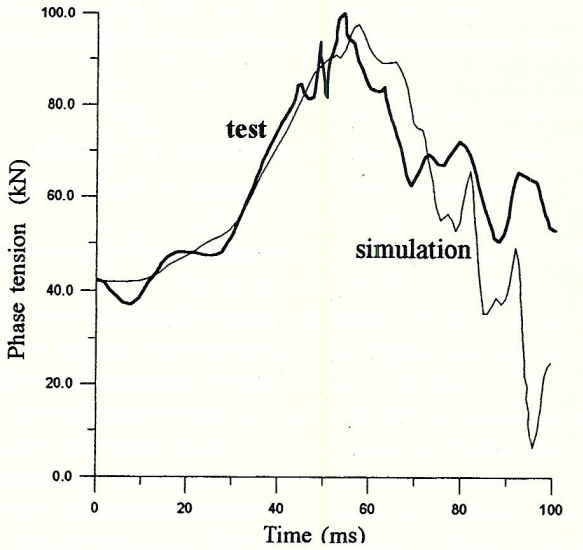

Fig. 6. Phase tension over the first 100 ms after short circuit inception; comparison of test (bold curve) and simulation with the data of Fig. 3.

the actual phenomenon, the transient behavior must be also well reproduced and understood.

In Figs. 5 and 6, such comparisons are presented for the spacer compression and the pinch force in the case of the 20 m and 40 kN test arrangement (test no. 4 from Table I).

Its is interesting to notice that in these tests, maximum spacer compression (occurring after 70 ms) is not simultaneous with the maximum tension in the conductor (occurring after 60 ms). This has a sensible impact on the spacer compression which is related to the instantaneous value of the conductor tension. This effect is very well reproduced by the computer simulation performed here.

V. Conclusions

Spacer compression during short-circuit has to be considered separately for overhead lines and substations. Typical subspan lengths (the part of the span between two spacers) are quite different (2–20 m in substations, 40–80 m in overhead lines). Spacing between subconductors is also sometimes different and mechanical tension in the conductors is generally much higher in overhead lines. These factors affect contact time (time needed to get the first contact between conductors), speed of traveling waves, contact length, etc., and thus influence sensibly spacer compression.

Spacer compression can be evaluated with a high degree of accuracy (±10%) by advanced calculation methods, if the data of the arrangement are sufficiently well known.

The Manuzio formula, mostly used today for spacer design, can induce in applications for substations up to 50% undervaluation error on the design load of the spacer, as shown for the configuration and short-circuit level examined here.

Correlation of computer simulation, is in very good agreement with the short subspans length configurations tested here, up to a short-circuit level of 40 kA rms (100 kA peak).

The order of magnitude for spacer compression is typically 15 kN for 40 kA, but it can be higher. Interestingly enough, short-circuit levels asked by some users are often very conservative (most of the short-circuits in most of the networks are much lower than 40 kA for one particular overhead line), but the situation could change in the next future when they could actually reach such high levels, because of increasing network interconnections. For this reason further developments are necessary in this field.

Although, as it has been shown in this paper, advanced calculation methods can solve the problem in the best way (i.e., with all effects included, access to transients, etc.), for daily design work and also for consideration in the relevant IEC standards and CIGRE recommendations, a simplified approach is required, a task which should be pursued in the near future.

Acknowledgment

The authors gratefully acknowledge the contribution of N. Stein of FGH to the execution of the tests.

REFERENCES

[1] C. Manuzio, "An investigation of the forces on bundle conductor spacers under fault conditions," *IEEE Trans. on PAS*, vol. PAS-86, no. 2, pp. 166–185, 1965.

[2] IEC 11/113/CD, "Overhead lines—Requirements and tests for spacers,", Committee Draft, 1996.

[3] "The mechanical effects of short-circuit currents in open-air substations (rigid and flexible bus-bars)," CIGRE, Paris, CIGRE Brochure no. 105, vols. 1 and 2, Apr. 1996.

[4] "Short-circuit currents—Calculation of effects, Part 1: Definitions and calculation methods,", CEI/IEC 865-1:1993.

[5] J. L. Lilien, "Contraintes et consequences electromecaniques liées au passage d'une intensité de courant dans les structures en cable," Ph.D. thesis, Collection des Publications de l'Université de Liège no. 87, Faculté des Sciences Appliquées, Liège, 1983.

Jean-Louis Lilien was born in Liège, Belgium on May 24, 1953. He received the degree in electrical and mechanical engineering in 1976 and the Ph.D. degree in 1984 from the University of Liège. He is presently a Professor at the same University, in the Department of Transmission and Distribution of Electrical Energy. He is the Chairman of the CIGRE task force on the effects of short-circuits in substations and he is an expert of the CIGRE task force on galloping. He has published more than 60 technical papers and has received the international prize "George Montefiore" in 1986.

Konstantin O. Papailiou was born in Athens, Greece on July 3, 1946. He received the electrical engineering degree from the Technical University of Braunschweig, the civil engineering degree from the University of Stuttgart and the Ph.D. degree from the Swiss Federal Institute of Technology (ETH) Zörich. He became engaged in transmission line work and high voltage engineering in 1975 as Director of R&D and the Overseas Division of GEA in Fellbach, Germany. Since 1986, he has been the Managing Director of SEFAG AG in Malters, Switzerland. He is member of various working groups of CIGRE, IEC, CENELEC, and SEV and has published several papers in this field.

Eric Hansenne was born in Liège, Belgium on June 18, 1970. He received the degree in electrical and mechanical engineering from the University of Liège in 1993. He presently works as a Researcher with Prof. Lilien. His main activity is based on short-circuit mechanical effects in substation structures.

Jürgen Kempf was born in Bad Mergentheim, Germany on August 30, 1958. He received the engineering degree (Dipl. Ing. FH) from the Fachhochschule Aalen. From 1985–1990, he worked as a Mechanical Engineer at the Physics Centre of the Fachhochschule Aalen. In 1990, he joined PFISTERER where he is responsible for mechanical testing. Mr. Kempf is a German Delegate to the WG09 of IEC TC 11.

Effect of Elevated Temperatures on Mechanical Properties of Overhead Conductors Under Steady State and Short-Circuit Conditions

Franc Jakl, *Member, IEEE,* and Andrej Jakl

***Abstract*—The loss of mechanical properties of conductors of transmission overhead lines is, from the point of view of their thermal stressing, the function of temperature and time of duration. Elevated temperatures generally result into the loss of the tensile strength of conductors which indirectly leads to increased sag and decreased safety heights or ground clearances, thus reducing the operational reliability of transmission lines. The paper presents results of a research into mechanical properties of hard-drawn wires and stranded homogeneous and combined conductors made of aluminum and aluminum-alloys at elevated temperatures under conditions of the steady-state operation. Further, results are shown of the changes of mechanical properties of such conductors as a result of short-circuit heating.**

***Index Terms*—Ground wires, hard-drawn wires, overhead conductors, sag, short circuit, steady state, temperature, tensile strength, unsteady state.**

I. Introduction

TECHNICAL and economical reasons are inducing managers and designers of electric power transmission systems to utilize the current-carrying components of the systems as fully as possible. Among these components are the transmission lines, and in particular the overhead conductors. Recently, environmental considerations are being paid much attention.

Increasing the thermal capacity of existing lines involves the study of changes in mechanical properties of conductor material due to high temperature operation in steady state and in special emergency events, particularly short circuits.

II. Research into the Mechanical Properties of Conductors at Elevated Temperatures in the Steady State

Both temperature and time of the heated state reflect themselves in the change of the conductor mechanical properties. The purpose of the research was to establish the loss of tensile strength of hard-drawn aluminum and aluminum-alloy wires and stranded conductors at various temperatures.

A. Experimental Work

Our experimental laboratory research into the mechanical properties of hard-drawn wires of Al 99.5 aluminum and AlMglE aluminum-alloy, mechanically similar to "6201" aluminum-alloy, was performed with a breaking device in a special thermal chamber equipped with a temperature control within the accuracy range of ±1°C. The length of testing tubes was 250 mm, length of the span was 150 mm, and base length for the calculation of the relative elongation was 50 mm. The rate of elongation was 2 mm/min which corresponds to the stressing speed of 7 $\mathrm{Nmm^{-2}s^{-1}}$. Prior to each measurement, all the samples were thermostated for 12 h in a thermal chamber in order to attain the necessary required temperatures, and were not tensioned during the thermostated period. They were then further thermostated for another 15 min after having been set between the jaws of a breaking device. Wire samples were taken from ACSR and AACSR conductors, manufactured according to DIN 48 204 standards.

The research into mechanical properties of completely stranded conductors under steady-state conditions was made under laboratory conditions on a special breaking device equipped with a hydraulic drive. The conductor heating up under the unloaded state was made with a DC current. The heating up time was 2 h. The tension clamps were isolated from the remaining construction and were compressed on the ends of a 6.5 m long of ACSR or AACSR conductors [1].

B. Experimental Results

The research carried out on hard-drawn wires made of Al 99.5 aluminum of the 3.44 mm diameter and on hard-drawn wires made of AlMglE aluminum-alloy of the 3.20 mm diameter proved that the loss of the tensile strength under the steady state at the $20°C \leq \vartheta \leq 100°C$ interval was in the case of Al 99.5 aluminum some 8.8% (in the elastic area some 4.6%) and in the case of AlMglE aluminum-alloy it was some 4.1% (in the elastic area some 5.9%). In the $80°C \leq \vartheta \leq 100°C$ interval, these values attain some 2.3% for Al 99.5 aluminum (in the elastic area some 0.9%) and in the case of AlMglE aluminum-alloy some 2.6% (in the elastic area some 2.5%, see Tables I and II). Table III shows the percentile loss into the mechanical properties of hard-drawn wires made of Al 99.5 aluminum in the temperature ranges from 80–120°C and from 80–150°C. In Tables I–IV, the meaning of symbols is as follows:

σ_m	tensile strength [$\mathrm{N/mm^2}$]
$\sigma_{p0.2}$	proof stress (nonproportional elongation) at 0.2% [$\mathrm{N/mm^2}$]
σ_{lin}	stress in elastic area (linear part of σ–ε diagram) [$\mathrm{N/mm^2}$]
ε	percentage elongation [%]

Manuscript received January 5, 1998; revised April 16, 1998.

F. Jakl is with the Faculty of Electrical Engineering, Computer Science and Information Technology, University of Maribor, Maribor, SI 2000 Slovenia.
A. Jakl is with ASD&S, Maribor, SI 2000 Slovenia.

Publisher Item Identifier S 0885-8977(00)00563-X.